Table II. Selected Bond Distances (Å) and Angles (deg) for $[(CO)_5Mn]_3Bi$ (**1**)

		(a) Distances			
Bi–Mn1	2.884 (1)	Bi–Mn2	2.916 (1)	Bi–Mn3	2.911 (1)
Mn1–C1	1.866 (8)	Mn2–C6	1.843 (7)	Mn3–C11	1.838 (7)
Mn1–C2	1.846 (8)	Mn2–C7	1.848 (8)	Mn3–C12	1.867 (8)
Mn1–C3	1.864 (7)	Mn2–C8	1.855 (8)	Mn3–C13	1.851 (7)
Mn1–C4	1.858 (7)	Mn2–C9	1.814 (7)	Mn3–C14	1.843 (6)
Mn1–C5	1.821 (7)	Mn2–C10	1.826 (7)	Mn3–C15	1.823 (7)
		(b) Angles			
Mn1–Bi–Mn2	110.3 (1)	Mn2–Bi–Mn3	106.9 (1)	Mn3–Bi–Mn1	107.5 (1)
Bi–Mn1–C1	85.0 (3)	Bi–Mn2–C6	84.5 (2)	Bi–Mn3–C11	79.1 (2)
Bi–Mn1–C2	83.4 (2)	Bi–Mn2–C7	83.0 (2)	Bi–Mn3–C12	82.0 (2)
Bi–Mn1–C3	84.7 (2)	Bi–Mn2–C8	86.4 (2)	Bi–Mn3–C13	86.4 (2)
Bi–Mn1–C4	90.8 (2)	Bi–Mn2–C9	175.6 (2)	Bi–Mn3–C14	96.8 (2)
Bi–Mn1–C5	176.5 (2)	Bi–Mn2–C10	95.8 (2)	Bi–Mn3–C15	170.7 (2)

undertook a crystallographic investigation of **1**. The determination of the structure of **1** would also provide valuable structural data for this scarcely investigated class of compounds.[11]

Diffraction-quality crystals were obtained from a saturated benzene solution of **1**, and the result of the analysis is shown in Figure 1. The atomic coordinates and equivalent isotropic thermal parameters are listed in Table I. Table II contains selected intramolecular bond distances and angles for **1**.

The monomeric **1** maintains a pyramidal geometry about the central bismuth atom, with each Mn atom having an approximate octahedral environment. The molecule relieves the possible steric interactions between the carbonyl groups of the $Mn(CO)_5$ units through conrotation about the three Mn–Bi vectors, such that the carbonyl ligands are interleaved. The average twist angle[13] of the four equatorial carbonyl ligands is 22.7°. The attainment of this relief results in the Mn–Bi–Mn′ angles being close to tetrahedral and only slightly greater than those found in $[(CO)_4Co]_3Bi$[7] (Co–Bi–Co′(av) = 106.8°). The conrotation of the $Mn(CO)_5$ units results in each molecule being chiral in the solid state; only one enantiomer is shown in Figure 1. The long Bi–Mn bonds also help to separate the manganese fragments, and in fact most of the Bi–Mn–C_{eq} angles are slightly less than 90°, indicating a distortion of the 12 equatorial carbonyl ligands *toward* the Bi atom. The axial carbonyl ligands show a shortening of 0.03 Å with respect to the equatorial carbonyls (averages: equatorial, 1.850 Å; axial, 1.819 Å), but all Mn–C–O angles are close to 180°, with no significant deviations from linearity.

Although structural data for first-row transition-metal–bismuth single bonds are scarce, the B–Mn distances in **1** (average 2.904 Å) are substantially longer than those for Bi–Co ($[(CO)_4Co]_3Bi$, Bi–Co(av) = 2.766 Å[7]) or those for Bi–Fe in open or closed clusters (e.g. in $\{[CpFe(CO)_2]_2BiCl\}_3$, Bi–Fe(av) = 2.687 (2) Å; $[BiFe_3(CO)_{10}]^-$, Bi–Fe = 2.650 (2) Å[8]). A dramatic difference in Bi–Mn bond lengths between **1** and the bismuthidene complex $\{[CpMn(CO)_2]_2BiCl\}_2$[4] also exists, where in the latter the dative Bi–Mn bond measures 2.469 Å. Comparative data for the heavy main-group elements Tl and Pb are also lacking[11] for cases where a single Mn–M bond is present. For the complexes $[(CO)_5Mn]_3M$, M = In,[14] Tl,[15] although synthesized, little reactivity has been explored. We can expect that these and the title compound should e.g. be photochemically active, providing routes to new closo cluster compounds incorporating heavy elements, as has been shown for iron.[9] Preliminary investigations indicate that intermediates in the reaction path leading to **1** are also isolable.

It is important to note that **1** does not crystallize from benzene as an arene adduct, while bismuth compounds with electronegative substituents have been found to form isolable π complexes with a variety of neutral arenes.[10]

Experimental Section

Synthesis of $[Mn(CO)_5]_3Bi$. The anion $Mn(CO)_5^-$ was prepared in thf solution (30 mL) from $Mn_2(CO)_{10}$ (0.69 g, 1.77 mmol) and sodium amalgam. The resulting solution was cooled to −30 °C, and a solution of $BiCl_3$ (0.19 g, 0.60 mmol) in thf (20 mL) was added dropwise over 15 min. The resulting golden brown solution was warmed to room temperature and evaporated to dryness under reduced pressure. The brown solid was washed with diethyl ether (3 × 25 mL) and the green residue recrystallized from CH_2Cl_2/ether (1:1), giving bright green needles: yield 0.45 g, 48%; mp 146 °C dec. IR (ν_{CO}, CH_2Cl_2, cm^{-1}): 2052 s, 2005 sh, 1978 vs. Anal. Calcd for $C_{15}BiMn_3O_{15}$ (M_r = 793.94): C, 22.69; O, 30.2; Mn, 20.76. Found: C, 22.69; O, 30.6; Mn, 20.76.

X-ray structure determination: Enraf-Nonius CAD4 diffractometer; $C_{15}BiMn_3O_{15}$, $M_r = 793.94$; monoclinic, $P2_1/n$; $a = 6.682$ (1), $b = 17.255$ (2), $c = 19.830$ (2) Å; $\beta = 99.22$ (1)°; $V = 2256.82$ Å^3; $D_{calcd} = 2.34$ g cm^{-3} for $Z = 4$; $F(000) = 1472$; μ(Mo Kα) = 91.16 cm^{-1}; 7282 measured reflections, 6546 unique ($R_{int} = 0.014$) and 4301 observed ($I \geqslant 2.0\sigma(I)$); ϑ–2ϑ scan, $\Delta\omega = 0.80 + 0.35 \tan\theta$, $[(\sin\theta)/\lambda]_{max} = 0.702$; *hkl* +9,+24,±27; Mo K$\alpha$ radiation, $\lambda = 0.71069$ Å; graphite monochromator. The data were corrected for decay, Lp, and absorption effects (empirical, relative transmission 0.67–1.00). Solution was by a novel random start multisolution direct methods program (SHELXS-86[16]) and was completed by Fourier syntheses. All atoms were refined anisotropically by full-matrix least squares, with $R = 0.033$, $R_w = 0.028$ ($w = 1/\sigma^2(F_o)$), 307 refined parameters, and $\Delta\rho_{final} = +0.99/1.06$ with a maximum at Bi (SHELX-76).

Acknowledgment. J.M.W. thanks the Royal Society (London) for a European Exchange Programme postdoctoral Fellowship.

Registry No. **1**, 106213-52-9; $Mn_2(CO)_{10}$, 10170-69-1; Mn, 7439-96-5; Bi, 7440-69-9.

Supplementary Material Available: Tables of complete distances and angles and anisotropic thermal parameters for **1** (4 pages); a table of observed and calculated structure factors for **1** (24 pages). Ordering information is given on any current masthead page.

---

[11] A recent review[12] indicates the absence of structural data for main-group–transition-element single bonds for most of the heavy group 14, 15, and 16 elements, in complexes of this type.

[12] Herrmann, W. A. *Angew. Chem.* **1986**, *98*, 57; *Angew. Chem., Int. Ed. Engl.* **1986**, *25*, 56.

[13] The twist angle gives a measure of the distortion from ideal C_{3v} symmetry. This angle is that between planes A and B. Plane A is defined by Bi, Mn, and the center of the Mn1, Mn2, and Mn3 triangle. Plane B is defined as Mn, the center of the 3 Mn triangle, and the two C_{eq} atoms closest to vertical. For C_{3v} symmetry this angle can be 0 or 45°.

[14] Hsieh, A. T. T.; Mays, M. J. *J. Chem. Soc., Dalton Trans.* **1972**, 516.

[15] Hsieh, A. T. T.; Mays, M. J. *Inorg. Synth.* **1976**, *16*, 61. Hsieh, A. T. T.; Mays, M. J. *J. Organomet. Chem.* **1970**, *22*, 29.

[16] Sheldrick, G. M., unpublished work, 1986.

Contribution from the Department of Chemistry,
University of Minnesota, Minneapolis, Minnesota 55455

Preparation of Gold Derivatives of Nitrido Clusters. Structural Characterization of $Ph_3PAuFeRu_3N(CO)_{12}$

Margaret L. Blohm[1] and Wayne L. Gladfelter*[2]

Received July 30, 1986

Although the first transition-metal compounds containing $AuPR_3$ groups were synthesized over 20 years ago,[3] this area has

Table I. Spectroscopic Data

compound	color	^{15}N chem shift (CH_2Cl_2), ppm	ν_{CO} (hexane), cm^{-1}
$Ph_3PAuFeRu_3N(CO)_{12}$	red	533.0	2084 w, 2060 vw, 2048 s, 2040 vs, 2024 m, 2008 m, 1995 w, 1979 vw
$Ph_3PAuRu_4N(CO)_{12}$	orange	492.4	2085 w, 2057 s, 2038 vs, 2028 w, 2009 s, 1999 w, 1989 vw, 1976 vw, 1967 vw
$Ph_3PAuFe_4N(CO)_{12}$	green-brown	592.9	2079 w, 2054 w, 2040 vs, 2025 vs, 2003 s, 1992 w, 1959 vw, 1944 vw

recently undergone substantial growth. Part of the interest in synthesizing gold derivatives of cluster compounds stems from the isolobal analogy between PR_3Au^+ and H^+.[4] The interaction of both H^+ and PPh_3Au^+ with carbido clusters of iron and ruthenium has led to products containing direct C–H and C–Au bonds, respectively.[5-12] We have reported the direct protonation of the nitrogen in nitrido clusters[13-15] and describe here the analogous reactions with the gold phosphine cation.

Experimental Section

$PPN[Fe_4N(CO)_{12}]$,[16] [PPN = bis(triphenylphosphine)nitrogen(1+) cation] $PPN[FeRu_3N(CO)_{12}]$,[17] $PPN[Ru_4{}^{15}N(CO)_{12}]$[18] and $PPN[NO_2]$[19] were prepared according to literature procedures. Ph_3PAuCl and $TlPF_6$ were purchased from Strem Chemicals. Tetrahydrofuran (THF) and diethyl ether were distilled from sodium benzophenone ketyl under nitrogen, and hexane was dried by distillation from sodium metal under nitrogen. Methylene chloride was distilled from P_2O_5 immediately prior to use, and all reactions were carried out under N_2 atmosphere. Infrared spectra were recorded on a Beckman Model No. 4250 spectrophotometer or a Mattson Cygnus 25 FTIR spectrophotometer equipped with a HgCdTe detector. NMR data were recorded on a Nicolet NTCFT-1130 300-MHz spectrophotometer. Each ^{15}N NMR experiment was conducted with CH_2Cl_2 as the solvent (3.0 mL) in a 12-mm tube with $Cr(acac)_3$ (53 mg) as the shiftless relaxation reagent. Nitromethane was used as an external reference, set at 379.60 ppm downfield from NH_3 (liquid, 25 °C).[20] The spectral data are summarized in Table I.

Preparation of $Ph_3PAuFeRu_3N(CO)_{12}$. CH_2Cl_2 (10 mL) was distilled into a Schlenk tube containing 100.9 mg of $PPN[FeRu_3N(CO)_{12}]$ (0.0809 mmol) and 44.0 mg of Ph_3PAuCl (0.0889 mmol). The solution was warmed to room temperature and stirred for 10 min or until the Ph_3PAuCl reagent had dissolved. The deep red solution was then transferred via a cannula into a second Schlenk tube containing 31.1 mg of $TlPF_6$ (0.0890 mmol). After 2 h, the reaction was complete and the CH_2Cl_2 was removed under vacuum. The residue was extracted with 2 × 10 mL of diethyl ether, and the red solutions were filtered. The solvent was removed from the filtrate and the product was extracted into 3 × 10 mL of hexane. The combined red-orange hexane solutions were then chromatographed with hexane as the eluent. Collection of the first band to elute, followed by removal of hexane solvent, led to the isolation of 74.4 mg (79%) $Ph_3PAuFeRu_3N(CO)_{12}$ as orange-red crystals. Anal. Calcd for $C_{30}H_{15}AuFeNO_{12}PRu_3$: C, 30.86; H, 1.30; N, 1.20. Found: C, 30.83; H, 1.33; N, 1.18.

Table II. Summary of Crystallographic Data

Crystal Parameters	
cryst syst	orthorhombic
space group	*Pbca*
formula	$C_{30}H_{15}AuFeNO_{12}PRu_3$
fw	1168.7
a, Å	16.977 (4)
b, Å	16.980 (4)
c, Å	24.872 (25)
V, Å^3	7170 (11)
Z	8
ρ(calcd), g cm^{-3}	2.17
temp, °C	24
abs coeff, cm^{-1}	57.83
cryst dimens, mm	0.45 × 0.25 × 0.04
trans factors (max–min), %	100–42.3
abs cor applied	empirical (ψ scans)
Measurement of Intensity Data	
diffractometer	Enraf-Nonius CAD-4
radiation	Mo Kα (λ = 0.71073 Å)
monochrometer	graphite crystal
programs used	Enraf-Nonius CAD-4-SDP programs
method of structure solution	heavy-atom method
scan type	ω–2θ
scan range, deg	$0 \leq 2\theta \leq 54$
reflcns measd	$+h,+k,+l$
no. of unique reflcns	3229
no. of reflcns used	2877
cutoff	$F_0 \geq 2.0\sigma(F_0)$
p	0.05
extinction coeff	1.038×10^{-8}
R	0.051
R_w	0.051
error in observn of unit wt	1.150

Preparation of $Ph_3AuRu_4N(CO)_{12}$. CH_2Cl_2 (10 mL) was distilled into a Schlenk tube containing $PPN[Ru_4N(CO)_{12}]$ (50.8 mg, 0.0384 mmol) and Ph_3PAuCl (21.0 mg, 0.0424 mmoles). After being warmed to room temperature, the solution was stirred for 20 min and then transferred, by cannula, to a second Schlenk tube containing $TlPF_6$ (14.8 mg, 0.0424 mmol). The procedure, similar to that used for $Ph_3PAuFeRu_3N(CO)_{12}$, gave a 62% yield of $Ph_3AuRu_4N(CO)_{12}$. Anal. Calcd for $C_{30}H_{15}AuNO_{12}PRu_4$: C, 29.70; H, 1.25; N, 1.15. Found: C, 29.39; H, 1.62; N, 1.13.

Preparation of $Ph_3PAuFe_4N(CO)_{12}$. $PPN[Fe_4N(CO)_{12}]$ (60.3 mg, 0.0549 mmoles) and Ph_3PAuCl (29.9 mg, 0.0604 mmoles) were dissolved in 10 mL of CH_2Cl_2. The resulting solution was transferred into a second Schlenk tube, which had been charged with 21.1 mg of $TlPF_6$ (0.0604 mmoles). After the dark brown solution was stirred at room temperature for 12 h, the solvent was evaporated under vacuum. At this point the procedure is the same as with $Ph_3PAuFeRu_3N(CO)_{12}$, yielding $Ph_3PAuFe_4N(CO)_{12}$ in 53% yield. Anal. Calcd for $C_{30}H_{15}AuFe_4NO_{12}P$: C, 34.89; H, 1.46; N, 1.36. Found: C, 35.52; H, 1.53; N, 1.33.

$Ph_3PAuFeRu_3N(CO)_{12}$ + PPN[X] (X = Cl, NO_2). THF (5 mL) was added to a Schlenk tube containing both $Ph_3PAuFeRu_3N(CO)_{12}$ (24.2 mg; 0.0207 mmol) and PPN[X] (X = Cl, 11.9 mg or X = NO_2, 12.1 mg, 0.0207 mmol). The color of the solution darkened immediately. The solution was stirred at room temperature for 30 min, after which the THF was removed under vacuum. Extraction of the solid with 2 × 5 mL diethyl ether, followed by filtration and layering of the filtrate with hexane, led to the isolation of crystalline $PPN[FeRu_3N(CO)_{12}]$ as the only product. An infrared spectrum in THF indicated that only one of the two possible isomers was present;[14] the product $PPN[FeRu_3N(CO)_{12}]$ contained the iron atom exclusively in the wing tip position.

X-ray Crystallographic Study. Red crystals of $Ph_3PAuFeRu_3N(CO)_{12}$ were grown by slow cooling of a concentrated hexane solution of the cluster. Details of the structural analysis (Table II) are similar to those of closely related compounds studied in our laboratory.[17] The systematic absences at (0*kl*, *k* = 2*n* + 1; *h*0*l*, *l* = 2*n* + 1; *hk*0, *h* = 2*n* + 1) were consistent with *Pbca*. Examination of the intensity of the appropriate reflections ruled out the possibility of a tetragonal crystal system despite

---

(1) National Science Foundation Predoctoral Fellow (1982–1985).

(2) Fellow of the Alfred P. Sloan Foundation (1983–1985).

(3) Coffey, C. E.; Lewis, J.; Nyholm, R. S. *J. Chem. Soc.* **1964**, 1741.

(4) Hoffmann, R. *Angew. Chem., Int. Ed. Engl.* **1982**, *21*, 711.

(5) Tachikawa, M.; Muetterties, E. L. *J. Am. Chem. Soc.* **1980**, *102*, 4541.

(6) Hriljac, J. A.; Swepston, P. N.; Shriver, D. F. *Organometallics* **1985**, *4*, 158.

(7) Davis, J. H.; Beno, M. A.; Williams, J. M.; Zimmie, J.; Tachikawa, M.; Muetterties, E. L. *Proc. Natl. Acad. Sci. U.S.A.* **1981**, *78*, 668.

(8) Holt, E.; Whitmire, K. H.; Shriver, D. F. *J. Am. Chem. Soc.* **1982**, *104*, 5621.

(9) Johnson, B. F. G.; Kaner, D. A.; Lewis, J.; Raithby, P. R.; Rosales, M. J. *J. Organomet. Chem.* **1982**, *231*, C59.

(10) Cowie, A. G.; Johnson, B. F. G.; Lewis, J.; Raithby, P. R. *J. Chem. Soc., Chem. Commun.* **1984**, 1710.

(11) Johnson, B. F. G.; Kaner, D. A.; Lewis, J.; Rosales, M. J. *J. Organomet. Chem.* **1982**, *238*, C73.

(12) Horwitz, C. P.; Holt, E. M.; Shriver, D. F. *J. Am. Chem. Soc.* **1985**, *107*, 281.

(13) Blohm, M. L.; Fjare, D. E.; Gladfelter, W. L. *J. Am. Chem. Soc.* **1986**, *108*, 2301.

(14) Blohm, M. L.; Gladfelter, W. L. *Organometallics* **1986**, *5*, 1049.

(15) Gladfelter, W. L. *Adv. Organomet. Chem.* **1985**, *24*, 41.

(16) Fjare, D. E.; Gladfelter, W. L. *Inorg. Chem.* **1981**, *20*, 3533.

(17) Fjare, D. E.; Gladfelter, W. L. *J. Am. Chem. Soc.* **1984**, *106*, 4799.

(18) Blohm, M. L.; Gladfelter, W. L. *Organometallics* **1985**, *4*, 45.

(19) Martinsen, A.; Songstad, J. *Acta Chem. Scand., Ser. A* **1977**, *A31*, 645.

(20) Levy, G. C.; Lichter, R. L. *Nitrogen-15 Nuclear Magnetic Resonance Spectroscopy*; Wiley: New York, *1979*.

Table III. Positional Parameters

atom	x	y	z
Au	0.10302 (4)	0.22121 (4)	0.11257 (2)
Fe1	0.1927 (1)	0.2836 (1)	0.25436 (8)
Ru2	0.11675 (9)	0.07952 (9)	0.26354 (5)
Ru3	0.20728 (7)	0.15882 (9)	0.18668 (5)
Ru4	0.05806 (7)	0.21759 (9)	0.21898 (5)
P	0.0645 (3)	0.2566 (3)	0.0278 (3)
C1A	−0.021 (1)	0.320 (1)	0.0268 (7)
C2A	−0.026 (1)	0.384 (1)	−0.0083 (8)
C3A	−0.096 (1)	0.429 (2)	−0.011 (1)
C4A	−0.154 (1)	0.413 (2)	0.024 (1)
C5A	−0.153 (1)	0.346 (1)	0.0584 (8)
C6A	−0.085 (1)	0.304 (1)	0.0595 (8)
C1B	0.0383 (9)	0.174 (1)	−0.0131 (6)
C2B	0.0867 (9)	0.107 (1)	−0.0126 (6)
C3B	0.069 (1)	0.044 (1)	−0.0430 (7)
C4B	0.003 (1)	0.041 (1)	−0.0754 (7)
C5B	−0.047 (1)	0.108 (1)	−0.0761 (7)
C6B	−0.028 (1)	0.172 (1)	−0.0453 (7)
C1C	0.1417 (9)	0.306 (1)	−0.0103 (6)
C2C	0.197 (1)	0.052 (1)	0.0163 (7)
C3C	0.257 (1)	0.391 (7)	−0.0113 (7)
C4C	0.261 (1)	0.380 (1)	−0.0656 (7)
C5C	0.207 (1)	0.337 (1)	−0.0928 (7)
C6C	0.146 (1)	0.299 (1)	−0.0653 (7)
N	0.1566 (7)	0.1835 (8)	0.2607 (5)
C11	0.290 (1)	0.287 (1)	0.2794 (8)
O11	0.3500 (9)	0.289 (1)	0.3009 (6)
C12	0.204 (1)	0.363 (1)	0.2099 (9)
O12	0.2107 (9)	0.417 (1)	0.1803 (6)
C13	0.150 (1)	0.339 (1)	0.3055 (7)
O13	0.1234 (8)	0.3704 (9)	0.3438 (6)
C21	0.048 (1)	0.069 (1)	0.3215 (7)
O21	0.0060 (8)	0.0667 (9)	0.3579 (6)
C22	0.071 (1)	−0.006 (1)	0.2269 (9)
O22	0.044 (1)	−0.060 (1)	0.2059 (7)
C23	0.190 (1)	0.016 (1)	0.2959 (8)
O23	0.2388 (9)	−0.016 (1)	0.3195 (6)
C31	0.263 (1)	0.225 (1)	0.1398 (6)
O31	0.3033 (8)	0.2630 (8)	0.1118 (5)
C32	0.301 (1)	0.113 (1)	0.2160 (8)
O32	0.3576 (7)	0.847 (8)	0.2296 (5)
C33	0.1884 (9)	0.075 (1)	0.1384 (6)
O33	0.1838 (7)	0.0228 (8)	0.1086 (5)
C41	−0.0172 (9)	0.154 (1)	0.1834 (7)
O41	−0.0630 (7)	0.1171 (8)	0.1616 (5)
C42	−0.005 (1)	0.237 (1)	0.2806 (7)
O42	−0.0447 (7)	0.2465 (8)	0.3167 (5)
C43	0.031 (1)	0.319 (1)	0.1901 (7)
O43	0.0147 (8)	0.3805 (8)	0.1744 (5)
Ru1	1.193	0.284	0.254
Fe2	1.117	0.080	0.264

the equivalent lengths of two axes. The check reflections showed no significant decay throughout the entire data collection.

After their initial location, the four metal atoms of the butterfly were labeled as ruthenium atoms, and their multiplicities were refined. The model was then changed to the real formula containing one iron atom and three ruthenium atoms, and from the multiplicities, the amount of iron and ruthenium were calculated at each site. The final occupancies located the iron atom exclusively in the wing tip positions and primarily in one of these, as labeled in Figure 1 [Fe1: Fe = 0.85, Ru = 0.15; Ru2: Fe = 0.15, Ru = 0.85]. The idealized positions for the hydrogen atoms were added to the list, but not refined, and the data set allowed anisotropic refinement for only the metal atoms and the phosphorus. The final difference Fourier map indicated no significant features. The values of the atomic scattering factors used in the calculations were taken from the usual tabulation,[21] and the effects of anomalous dispersion were included for the non-hydrogen atoms. The positional parameters, bond distances, and bond angles are listed in Tables III–V.

Results and Discussion

Formation of $Ph_3PAuM_4N(CO)_{12}$. By far the most common method of synthesizing gold derivatives of transition-metal clusters is the reaction of an anionic carbonyl species with R_3PAuX (X = Cl or NO_3^-).[22] When the less reactive R_3PAuCl is used, greater success is obtained when $TlPF_6$ is added to remove Cl^- and generate R_3PAu^+ in situ. As this particular method was the one used to enter both the tetrairon- and tetrarutheniumgold carbide systems, we chose it as the method for synthesizing the gold derivatives of iron and ruthenium nitrides.

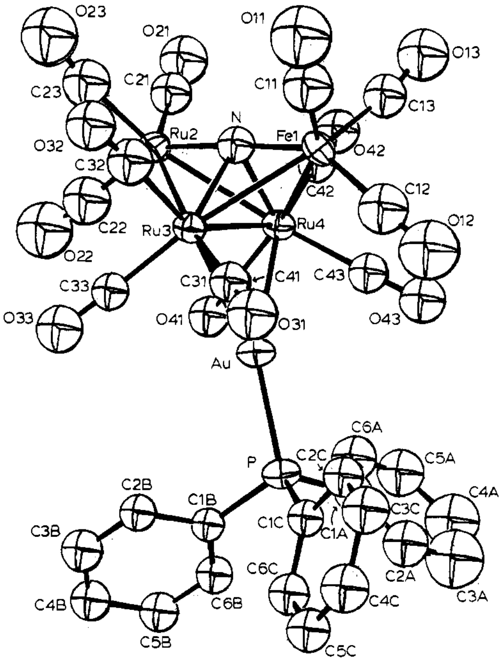

Figure 1. View of $Ph_3PAuFeRu_3N(CO)_{12}$ showing the atom labels. A small amount (15%) of disorder exists between the wing tip metals. The labels Fe1 and Ru2 are used to indicate the primary component at that site.

Table IV. Interatomic Distances for $(C_6H_5)_3PAuFeRu_3N(CO)_{12}$

atoms	dist, Å	atoms	dist, Å
	$FeRu_3N(AuP)$ Core		
Fe1–N	1.81 (1)	Ru3–N	2.08 (1)
Fe1–Ru3	2.717 (2)	Ru3–Ru4	2.839 (2)
Fe1–Ru4	2.693 (2)	Ru3–Au	2.766 (1)
Ru2–N	1.89 (1)	Ru4–N	2.05 (1)
Ru2–Ru3	2.798 (2)	Ru4–Au	2.755 (1)
Ru2–Ru4	2.778 (2)	Au–P	2.287 (4)
	Metal–Ligand Distances		
Fe1–C11	1.77 (2)	Ru3–C31	1.87 (2)
Fe1–C12	1.76 (2)	Ru3–C32	1.91 (2)
Fe1–C13	1.74 (2)	Ru3–C33	1.89 (2)
Ru2–C21	1.86 (2)	Ru4–C41	1.89 (2)
Ru2–C22	1.88 (3)	Ru4–C42	1.90 (2)
Ru2–C23	1.84 (2)	Ru4–C43	1.92 (2)
	Ligand Distances		
C11–O11	1.15 (2)	C31–O31	1.17 (2)
C12–O12	1.18 (2)	C32–O32	1.13 (2)
C13–O13	1.18 (2)	C33–O33	1.16 (2)
C21–O21	1.16 (2)	C41–O41	1.14 (2)
C22–O22	1.15 (3)	C42–O42	1.13 (2)
C23–O23	1.14 (2)	C43–O43	1.15 (2)

Each of the nitrides was found to react in a similar fashion with Ph_3PAuCl and $TlPF_6$ in CH_2Cl_2 to form TlCl, $PPN(PF_6)$, and the gold phosphine adduct of the metal cluster in yields ranging from 53 to 79%. Elemental analysis showed that each of the compounds had the same general formula, $Ph_3PAuM_4N(CO)_{12}$, and infrared spectroscopy established that the structures were similar within the series.

Literature precedents exist for structures **1**[9] and **2**,[10] shown below, where the gold is spanning either the wing tip metals or the hinge metals. The question regarding the location of the gold

---

[21] (a) Cromer, D. T.; Waber, J. T. *International Tables for X-ray Crystallography*; Kynoch: Birmingham, England, 1974; Vol. IV, Table 2.2A. Cromer, D. T. *Ibid.*; Table 2.3.1. (b) Cromer, D. T.; Ibers, J. A. *Ibid.*; Table 2.2C.

Table V. Selected Bond Angles for $Ph_3PAuFeRu_3N(CO)_{12}$

atoms	angle, deg	atoms	angle, deg
	$PAuFeRu_3N$ Core		
Ru3-Fe1-Ru4	63.30 (6)	Ru2-Ru4-Au	107.62 (6)
Ru3-Ru2-Ru4	61.21 (5)	Ru3-Ru4-Au	59.26 (4)
Fe1-Ru3-Ru2	84.36 (6)	Ru3-Au-Ru4	61.88 (4)
Fe1-Ru3-Ru4	57.94 (5)	Ru3-Au-P	153.8 (1)
Fe1-Ru3-Au	93.20 (6)	Ru4-Au-P	144.3 (1)
Ru2-Ru3-Ru4	59.05 (5)	Fe1-N-Ru2	176.9 (7)
Ru2-Ru3-Au	106.74 (5)	Fe1-N-Ru3	88.4 (5)
Ru4-Ru3-Au	58.87 (4)	Fe1-N-Ru4	88.1 (5)
Fe1-Ru4-Ru2	85.20 (6)	Ru2-N-Ru3	89.6 (5)
Fe1-Ru4-Ru3	58.76 (6)	Ru2-N-Ru4	89.4 (5)
Fe1-Ru4-Au	93.98 (6)	Ru3-N-Ru4	86.9 (4)
Ru2-Ru4-Ru3	59.74 (5)		
	Ligand-Metal-Ligand		
N-Fe1-C11	108.6 (8)	N-Ru3-C31	130.0 (6)
N-Fe1-C12	144.3 (8)	N-Ru3-C32	95.0 (7)
N-Fe1-C13	107.7 (7)	N-Ru3-C33	130.3 (6)
C11-Fe1-C12	95.4 (9)	C31-Ru3-C32	93.3 (7)
C11-Fe1-C13	96.3 (9)	C31-Ru3-C33	98.0 (7)
C12-Fe1-C13	95.1 (9)	C32-Ru3-C33	94.5 (8)
N-Ru2-C21	109.9 (7)	N-Ru4-C41	129.0 (6)
N-Ru2-C22	148.1 (8)	N-Ru4-C42	95.8 (6)
N-Ru2-C23	108.8 (8)	N-Ru4-C43	129.6 (6)
C21-Ru2-C22	92.6 (9)	C41-Ru4-C42	95.5 (7)
C21-Ru2-C23	91.7 (8)	C41-Ru4-C42	99.8 (8)
C22-Ru2-C23	92.2 (9)	C42-Ru4-C43	90.7 (8)
	Metal-Carbonyl		
Fe1-C11-O11	173 (2)	Ru3-C31-O31	175 (1)
Fe1-C12-O12	179 (2)	Ru3-C32-O32	175 (2)
Fe1-C13-O13	173 (2)	Ru3-C33-O33	174 (2)
Ru2-C21-O21	177 (2)	Ru4-C41-O41	179 (2)
Ru2-C22-O22	178 (2)	Ru4-C42-O42	177 (2)
Ru2-C23-O23	171 (2)	Ru4-C43-O43	178 (2)

phosphine in these nitrido clusters was not resolved by the spectral data alone.

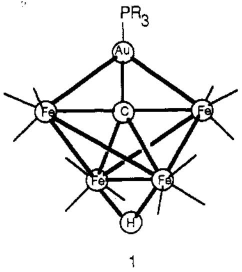

1

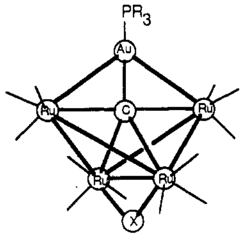

X = H, AuPR3 , I

2

A further structural ambiguity existed in the mixed-metal system that used the anion $[FeRu_3N(CO)_{12}]^-$ for the starting material. The recently reported[17] structure of $Et_4N[FeRu_3N(CO)_{12}]$ found that a mixture of two isomers cocrystallized; one isomer contained iron in the wingtip position, and the second isomer contained iron in the hinge position (**3** and **4**). While these isomers interconvert, they do so slowly on the laboratory time scale at 25 °C. When a mixture of these two isomers is protonated, the only product contains the iron atom exclusively in the wing tip position[13] and the hydride bridges a hinge Ru-Ru bond of $HFeRu_3N(CO)_{12}$ (**5**). This assignment was made on the basis of ^{13}C NMR data, since X-ray quality crystals of **5** could not be isolated.

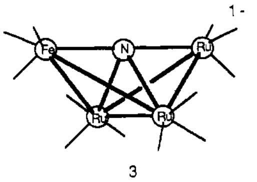

3

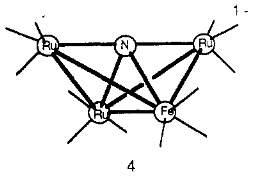

4

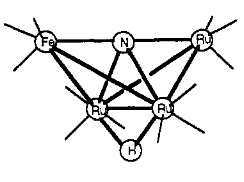

5

Structure of $Ph_3PAuFeRu_3N(CO)_{12}$. To address both of the above questions a single-crystal X-ray crystallographic analysis of $Ph_3PAuFeRu_3N(CO)_{12}$ was completed. The structure, shown in Figure 1, contains four $M(CO)_3$ groups in a butterfly arrangement with the nitrogen atom coordinated to all four metal atoms. Selected bond distances and angles are given in Tables IV and V. In contrast to the starting anion, the iron atom of $Ph_3PAuFeRu_3N(CO)_{12}$ was located exclusively in the wing tip position of the butterfly. The structurally characterized $Et_4N[FeRu_3N(CO)_{12}]$, contained 74% iron in the wing tip positions and 26% iron in the hinge positions. The occupancy of the iron atom in the neutral gold cluster was refined to 85% in one unique wing tip site. The dihedral angle between the Fe1-Ru3-Ru4 and Ru2-Ru3-Ru4 planes is 104°, only a slight increase from the corresponding 101° angle in the anionic nitride.[17] As in other tetrametal nitrido clusters,[15] the contacts between the nitrogen and wing tip metals are shorter (Fe1-N, 1.81 (1) Å; Ru2-N, 1.89 (1) Å) than those to the metals in the hinge position (Ru3-N, 2.08 (1) Å; Ru4-N, 2.05 (1) Å. The coordination geometry about the nitrogen atom is close to octahedral, with two vacant cis sites. The Fe1-N-Ru2 bond angle is nearly linear at 176.9°, virtually identical with the value of 176.6° found for $Et_4N[FeRu_3N(CO)_{12}]$.[17]

The gold atom symmetrically bridges the hinge ruthenium-ruthenium bond. As is generally observed for metal-metal bonds bridged by a gold ligand,[22] the bond has been lengthened substantially (2.839 (2) Å) relative to the hydride-bridged hinge ruthenium-ruthenium bond of 2.804 (1) Å in $HRu_4N(CO)_{11}P(OMe)_3$[23] and the unbridged bond of 2.672 (1) Å in $[Ru_4N(CO)_{12}]^-$.[24] The Ru-Au bond lengths of 2.766 (1) and 2.755 (1) Å are typical for 3-center 2e gold-bridged Ru-Ru bonds.[9,25-29] An unusual feature present in $Ph_3PAuFeRu_3N(CO)_{12}$ is the observed 11° tilt of the Ru3-Au-Ru4 plane, relative to the Ru3-N-Ru4 plane, toward the wing tip iron atom. The position of the gold atom has forced a distortion of the carbonyl ligands cis to the gold atom on the hinge metals. All other parameters associated with the twelve linear carbonyls are normal. The bond angles and lengths of the $Au-PPh_3$ ligand are typical of similarly coordinated gold ligands,[22] with a Au-P bond distance of 2.287 (4) Å.

^{15}N NMR Study. ^{15}N NMR spectroscopy is a sensitive and informative tool in characterizing cluster nitrides.[15] Specifically, an interesting trend has been observed between M_4N^- butterfly clusters and their hydride derivatives, HM_4N; the ^{15}N chemical shift of the anion is approximately 28 ppm upfield of the neutral hydride.[15-18] Hoping to gain more information about the structures of the tetrairon and tetraruthenium gold clusters, we synthesized the ^{15}N-labeled derivatives of the three compounds.

Table I summarizes the ^{15}N data for the gold species. The structure of $Ph_3PAuFeRu_3N(CO)_{12}$ has the PPh_3Au group in the same position proposed for the hydride in $HFeRu_3N(CO)_{12}$. The

---

(22) Hall, K. P.; Mingos, D. M. P. *Prog. Inorg. Chem.* **1984**, *32*, 237.
(23) Braga, D.; Johnson, B. F. G.; Lewis, J.; Mace, J. M.; McPartlin, M.; Puga, J.; Nelson, W. J. H.; Raithby, P. R.; Whitmore, K. H. *J. Chem. Soc., Chem. Commun.* **1982**, 1081.
(24) Blohm, M. L.; Gladfelter, W. L., unpublished results.
(25) Bateman, L. W.; Green, M.; Mead, K. A.; Mills, R. M.; Salter, I. D.; Stone, F. G. A.; Woodward, P. *J. Chem. Soc., Dalton Trans.* **1983**, 2599.
(26) Bateman, L. W.; Green, M.; Howard, J. A. K.; Mead, K. A.; Mills, R. M.; Salter, I. D.; Stone, F. G. A.; Woodward, P. *J. Chem. Soc., Chem. Commun.* **1982**, 773.
(27) Freeman, M. J.; Green, M.; Orpen, A. G.; Salter, I. D.; Stone, F. G. A. *J. Chem. Soc., Chem. Commun.* **1983**, 1332.
(28) Bruce, M. I.; Nicholson, B. K. *J. Organomet. Chem.* **1983**, *252*, 243.
(29) Mays, M. J.; Raithby, P. R.; Taylor, P. L.; Henrick, K. *J. Organomet. Chem.* **1982**, *224*, C45.

similarity in structure is also reflected in ^{15}N chemical shift; $HFeRu_3{}^{15}N(CO)_{12}$[17] and $Ph_3PAuFeRu_3{}^{15}N(CO)_{12}$ resonate at 530.9 and 533.0 ppm, respectively, a difference in chemical shift of only 2.1 ppm. The shifts of the two gold homonuclear clusters are also approximately 2 ppm downfield from the corresponding hydrides. These facts along with the IR data suggest the gold is also bridging the hinge M–M bonds in $Ph_3PAuFe_4N(CO)_{12}$ and $Ph_3PAuRu_4N(CO)_{12}$.

Removal of the Gold Phosphine Group. The three new compounds were reacted with $PPN(NO_2)$ in an attempt to synthesize new nitrido–nitrosyl clusters. We found, however, that reaction occurred immediately, not only wth $PPN(NO_2)$, but also with PPNCl, to remove the Ph_3PAu group from the cluster. Such reactivity is not unprecedented, as $[HBEt_3]^-$ and I^- have been used as a nucleophilic reagent to remove the gold ligand from other carbonyl clusters.[9]

Acknowledgment. This research was supported by a grant from the National Science Foundation (No. CHE-8410999).

Supplementary Material Available: Tables of isotropic and anisotropic thermal parameters and complete distances and angles (8 pages); calculated and observed structure factors (12 pages). Ordering information is given on any current masthead page.

Contribution from the Departments of Chemistry,
University of Delaware, Newark, Delaware 19716,
and Rice University, Houston, Texas 77251

Synthesis and Characterization of a Double-Spiro μ_4-Antimony Metal Carbonyl Complex, $[Fe_2(CO)_8(\mu_4\text{-}Sb)]_2[Fe_2(CO)_6]$

Arnold L. Rheingold,*[†] Steven J. Geib,[†] Minghuey Shieh,[‡]
and Kenton H. Whitmire*[‡]

Received August 1, 1986

Examples of clusters containing single "bare" or "naked" group 15 atoms (E) bridging transition-metal atoms have recently become more numerous.[1] However, the number of structurally confirmed examples in which the E atom links four or more metal atoms remains small. Examples include μ_4-spiro complexes $[Fe_2(CO)_8EFe_2(CO)_6Cl]$, E = P or As,[2] $[Co_4(\eta^5\text{-}C_5H_5)_4(CO)_4(\mu_4\text{-}As)]BF_4$,[3] one μ_6-As structure, $[Co_8(\mu_6\text{-}As)(\mu_4\text{-}As)(\mu_4\text{-}AsPh)_2(CO)_{16}]_2$,[4] and a few examples of partial[5] or complete encapsulation.[6] The isolobal analogy between E and CH makes understandable the more common μ_3-E, triangular-face capping properties of E atoms.[7]

Except for the encapsulated Sb atom in $[Rh_{12}Sb(CO)_{27}]^{3-}$,[6] no clusters containing four or more metal atoms linked by an Sb atom are known. In fact antimony atom clusters of any type are extremely rare; the only previously reported cluster is $Sb_2[W(CO)_5]_3$.[8] We now report the synthesis and characterization of $[Fe_2(CO)_8(\mu_4\text{-}Sb)]_2[Fe_2(CO)_6]$ (**1**) containing two spirolike μ_4-Sb(Fe_4) linkages.

Experimental Section

Synthesis of $[Fe_2(CO)_8(\mu_4\text{-}Sb)]_2[Fe_2(CO)_6]$ (1). Compound **1** was obtained by first treating 6.14 g of $[Et_4N]_2[Fe_2(CO)_8]$[9] (10.3 mmol) with 1.55 g of $SbCl_3$[10] (6.8 mmol) in dried acetone. This yielded a reddish brown solution, which was filtered and treated with 4.31 g of $[Cu(CH_3CN)_4][BF_4]$.[11] After being stirred overnight, the dark brown solution was filtered to remove precipitated copper and the solvent removed under vacuum. The solid residue was extracted into CH_2Cl_2/toluene (1:3) and chromatographed on Florisil by eluting with toluene to give brown $Sb_2Fe_6(CO)_{22}$ (**1**) in 8.5% yield. **1** is insoluble in hexane but soluble in most common organic solvents. IR (ν_{CO}, CH_2Cl_2): 2110 sh, 2090 m, 2060 m, 2038 s, 1995 w, 1960 w cm^{-1}. Mp: 232–233 °C dec.

Table I. Crystal Data Collection and Refinement Data for $Sb_2Fe_6(CO)_{22}$

(a) Crystal Parameters			
formula	$C_{22}Fe_6O_{22}Sb_2$	Z	8
cryst system	orthorhombic	D(calcd), g cm^{-3}	2.27
space group	*Pbca*	μ, cm^{-1} (Mo Kα)	41.0
a, Å	18.016 (3)[a]	cryst size, mm	0.21 × 0.21 × 0.38
b, Å	16.414 (4)	color	deep red
c, Å	23.672 (6)	temp, °C	23
V, $Å^3$	7000 (3)		
(b) Data Collection			
diffractometer	Nicolet R3m/μ	data collected	$+h,+k,+l$
radiation	Mo Kα (λ = 0.71073 Å)	rflns collected	6113
		obsd rflns ($F_o \geq 4\sigma(F_o)$)	3949
monochromator	graphite	std rflns	3 std/97 rflns
scan method	omega	decay	<1%
2θ scan limits, deg	$4 \leq 2\theta \leq 48$	T_{max}/T_{min}	0.288/0.210
scan speed, deg min^{-1}	var, 5–20		
(c) Refinement			
R_F/R_{wF}, %	3.84/4.03	Δ/σ	0.075
g[b]	0.001	$\Delta\rho$(max), e $Å^{-3}$	0.58
GOF	1.009	$\Delta\rho$(min), e $Å^{-3}$	−0.49
data/param	8.40		

[a] Unit-cell parameters, least-squares best fit, angular settings of 25 reflections, $20° \leq 2\theta \leq 30°$. [b] $w^{-1} = \sigma^2(F_o) + gF_o^2$.

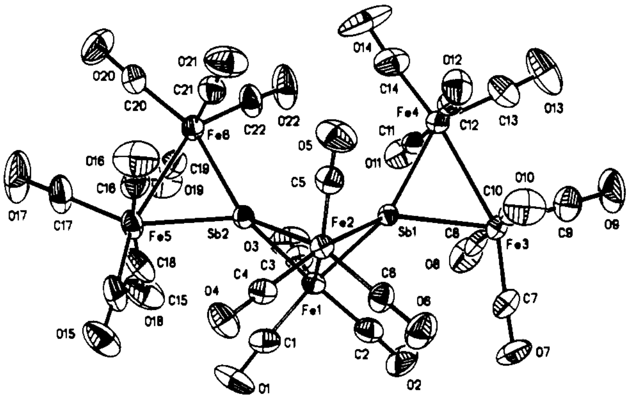

Figure 1. Molecular structure and labeling scheme for $[Fe_2(CO)_8(\mu_4\text{-}Sb)]_2[Fe_2(CO)_6]$ (**1**) with 45% probability thermal ellipsoids.

X-ray Structural Characterization. Crystals suitable for diffraction were recrystallized from CH_2Cl_2. Crystal data and parameters used

---

[†] University of Delaware.

[‡] Rice University.

(1) Herrmann, W. A. *Angew. Chem., Int. Ed. Engl.* **1986**, *25*, 56.

(2) Huttner, G.; Mohr, G.; Pritzlaff, B.; Von Seyerl, J.; Laszlo, Z. *Chem. Ber.* **1982**, *115*, 2044.

(3) Campana, C. F.; Dahl, L. F. *J. Organomet. Chem.* **1977**, *127*, 209.

(4) Rheingold, A. L.; Sullivan, P. J. *J. Chem. Soc., Chem. Commun.* **1983**, 39.

(5) $[Fe_4(\mu_4\text{-}N)(CO)_{12}]^-$: Fjare, D. E.; Gladfelter, W. L. *J. Am. Chem. Soc.* **1981**, *103*, 1572. $[Ru_5(CO)_{16}(\mu\text{-}PPh_2)(\mu_5\text{-}P)]$: MacLaughlin, S. A.; Taylor, N. J.; Carty, A. J. *Inorg. Chem.* **1983**, *22*, 1409.

(6) $[Rh_9P(CO)_{21}]^{2-}$: Vidal, J. L.; Walker, W. E.; Pruett, R. L.; Schoening, R. C. *Inorg. Chem.* **1979**, *18*, 129. $[Co_6P(CO)_{16}]^-$: Chini, P.; Ciania, G.; Martinengo, S.; Sironi, A.; Longhetti, L.; Heaton, B. T. *J. Chem. Soc., Chem. Commun.* **1979**, 188. $[Rh_{10}As(CO)_{22}]^{3-}$ and $[Rh_{12}Sb(CO)_{27}]^{3-}$: Vidal, J. *Inorg. Chem.* **1981**, *20*, 243. Vidal, J.; Troup, J. M. *J. Organomet. Chem.* **1981**, *213*, 351.

(7) Some examples of μ_3-E complexes are as follows. $[Co_3(CO)_9(\mu_3\text{-}P)]$: Vizi-Orosz, A.; Palyi, G.; Marko, L. *J. Organomet. Chem.* **1973**, *60*, C25. Vizi-Orosz, A. *J. Organomet. Chem.* **1976**, *111*, 61. $[Co_4(\eta^5\text{-}C_5H_5)_4(\mu_3\text{-}P)_4]$: Dahl, L. F.; Simon, G. L. *J. Am. Chem. Soc.* **1973**, *95*, 2175. $[Mo_4(\eta^5\text{-}C_5H_5)_4(\mu_3\text{-}As)_4]$: Rheingold, A. L.; Foley, M. J.; Sullivan, P. J. *J. Am. Chem. Soc.* **1982**, *104*, 4727. $[Fe_3(CO)_9(\mu_3\text{-}As)_2]$: Delbaere, L. T. J.; Kruczynski, L. J.; McBride, D. W. *J. Chem. Soc., Dalton Trans.* **1973**, 307. $[Co_4(\mu_3\text{-}As)_3(\mu_3\text{-}\eta^3\text{-}As_3)(PPh_3)_4]$: Fenske, D.; Hachgenei, J. *Angew Chem., Int. Ed. Engl.* **1986**, *25*, 175. $[Fe_3(CO)_9(\mu_3\text{-}Bi)_2]$: Whitmire, K. H.; Lagrone, C. B.; Churchill, M. R.; Fettinger, J. C.; Biondi, L. V. *Inorg. Chem.* **1984**, *23*, 4227.

0020-1669/87/1326-0463$01.50/0